

Hybrid Domain Evaluation PTS with Adaptive Selection Methods for PAPR Reduction

Feng Hu

communication university of china

Yuan Lu (✉ luyuancuc@cuc.edu.cn)

Communication University of China <https://orcid.org/0000-0002-6940-2935>

Libiao JIN

communication university of china

Jianbo Liu

Communication University of China

Zhiping Xia

Academy of Broadcasting Science

Guoting Zhang Zhang

Academy of Broadcasting Science

Jingting Xiao Xiao

Academy of Broadcasting Science

Research

Keywords: Multicarrier-system, 5G communication, partial transmission sequence, OFDM, power amplifier efficiency, PAPR

Posted Date: March 22nd, 2021

DOI: <https://doi.org/10.21203/rs.3.rs-331243/v1>

License:   This work is licensed under a Creative Commons Attribution 4.0 International License.

[Read Full License](#)

Version of Record: A version of this preprint was published at Energies on April 8th, 2022. See the published version at <https://doi.org/10.3390/en15082738>.

RESEARCH

Hybrid Domain Evaluation PTS with Adaptive Selection Methods for PAPR Reduction

Feng Hu¹, Yuan Lu¹, Libiao Jin^{1*}, JianBo Liu^{1*}, Zhiping Xia², Guoting Zhang² and Jingting Xiao²

*Correspondence:

libiao@cuc.edu.cn; libi@cuc.edu.cn

¹School of Information and Communication Engineering, Communication University of China, Beijing, China

Full list of author information is available at the end of the article

Abstract

Partial transmit sequence (PTS) technique is a fairly suitable scheme to mitigate the high peak-to-average power ratio (PAPR) problem inherent in 5G multicarrier system—especially considering high-order QAM modulation design. However, the high computational complexity level and the speed of the convergence for optimizing the phases of the transmitting signal restricts this technique in practical applications. In this paper, a low-complexity frequency domain evaluated PTS (F-PTS) based on spacing multi-objective (SMO) processing algorithm is proposed to reduce the PAPR values. The PAPR performance are accurately predicted in terms of modifying relative dispersion in the frequency domain. As a result, the complexity of searching the optimal phase factors and IFFT computing is simplified. Moreover, frequency domain and time domain evaluating PTS (FTD-PTS) is employed to search the optimal solution within reasonable complexity. Simulation results verify that the F-PTS scheme can obtain well secondary peaks with lower computational complexity, and the FTD-PTS scheme effectively reduces PAPR with a faster convergence speed.

Keywords: Multicarrier-system; 5G communication; partial transmission sequence; OFDM; power amplifier efficiency; PAPR

Introduction

Orthogonal frequency division multiplexing (OFDM) is one of the most representative multicarrier modulation (MCM) techniques due to its capability to efficiently cope with frequency selective channels for 5G broadband wireless communication[1]. However, OFDM is restricted by some obstacles such as the high peak-to-average-power ratio (PAPR)[2], which drives the OFDM signals to work in the nonlinear region of high-power amplifiers (HPA)[3] and this leads to appearing undesirable degradation in the Bit Error Rate (BER) performance [4]. An increase in back-off of HPA will lead to a loss in power efficiency, therefore, PAPR reduction is necessary and more efficient for energy optimization.

Various PAPR reduction schemes have been proposed to solve this issue, which are: distortion method, companding method, block coding, selective mapping (SLM)[5], and partial transmit sequence (PTS)[6]. Among all existing techniques, PTS is very promising for 5G waveform because of its efficient PAPR reduction performance without any signal distortion. The major drawback of PTS technologies is high computational complexity. To search for the optimal phase combination, large numbers of sub-blocks are inevitable, which increases searching complexity exponentially [7]. In low-complexity PTS methods, one of the most attractive methods is using dominant time-domain samples[8]. Unfortunately, a set of multi-point IFFT

operations using entire points calculate PAPR values, which significantly increases computational complexity, especially for PTS algorithm [9].

In this work, a new metric which can select dominant frequency-domain samples accurately is proposed. Specifically, we propose a novel method based on spacing multi-objective (SMO) processing algorithm to search a sub-optimal PTS scrambling signal[10]. The PAPR performance are accurately predicted in terms of modifying relative dispersion before IFFT operations. Then, the dominant complexity of IFFT computing is evaded. The proposed low-complexity F-PTS methods can achieve much lower computational complexity without degrading the PAPR reduction performance. We also show that SMO processing has a unique structure that can be exploited to implement the PTS efficiently. Thus, the second proposed scheme, FTD-PTS, may achieve an optimal solution within a faster convergence speed. SMO evaluating is conducted to prefer PTS subset before IFFT operations, instead of randomly selecting subset. Then, time-domain metrics are used to estimate the PAPR of each candidate signal after finding the preferred PTS subset. Then, time-domain metrics are used to estimate and designate the achievable optimal solution accurately, and remove part of samples from the procedure of preferred PTS subset. Compared with the conventional PTS method, the improved PTS method has the reasonable computational complexity and PAPR reduction can reach achievable lower bounds accurately.

OFDM system

In this section, OFDM structure and PAPR definition would be represented. The continuous-time baseband OFDM sequence can be expressed as:

$$x(t) = \sum_{k=0}^{N-1} X_k(t)e^{j2\pi k\Delta f t}, 0 \leq t \leq T \quad (1)$$

where N data symbols $\mathbf{X} = \{X_k, k = 0, 1, \dots, N - 1\}$ generated OFDM signals, which are chosen from phase-shift-keying (PSK) or quadrature amplitude modulation (QAM) constellation mapping, T represents OFDM signal duration, $\Delta f = 1/T$ is the frequency interval between subcarrier[11].

Likewise, the discrete-time baseband OFDM sequence with L times oversampling can be represented as:

$$x_n = \frac{1}{\sqrt{LN}} \sum_{k=0}^{N-1} X_k(t)e^{j2\pi nk/LN}, n=0, 1, \dots, LN - 1 \quad (2)$$

According to central limit theorem, for OFDM signals with massive subcarriers follow the Gaussian distribution, which amplitude follow Rayleigh distribution. Peak-to-Average Power Ratio (PAPR) is usually used to describe the characteristics of signal amplitude fluctuations, which occurs when different phase sub-carriers achieve the maximum amplitude simultaneously[12]. High PAPR will lead to HPA exceeds the dynamic range that caused nonlinear distortion. PAPR of L times over-

sampled OFDM signal could be defined as:

$$\text{PAPR} = 10 \log_{10} \left(\frac{\max_{0 \leq n \leq NL-1} [x_n]^2}{\underset{P_{avx}(n)}{\mathbb{E} [x_n]^2}} \right) \quad (3)$$

Complementary Cumulative Distribution Function (CCDF) is the major measure instrument to clarify the performance of PAPR in OFDM systems, which was defined as the probability that the PAPR ratio exceeds a certain threshold Z_0 [13].

$$\begin{aligned} \text{CCDF}_{\text{PAPR}}(\text{PAPR}_0) &= \Pr(\text{PAPR} > \text{PAPR}_0) \\ &= 1 - F(Z) \\ &= 1 - (1 - e^{-Z_0})^N \end{aligned} \quad (4)$$

1 PTS technique

High PAPR is a major obstacle to the high energy efficiency of MCM system in 5G communication [15]. By continuous signal sub-blocks and computational power consumption, PTS is a non-distortion method and one of the few PAPR reduction techniques applied in 5G high-order QAM scenarios communication [16].

1.1 PTS scheme

The principle of PTS is to reduce PAPR by scrambling partitioned sub-blocks into different phases. Fig. 1 depicts the scheme of PTS, where the input frequency-domain signal was divided into several sub-carriers, each of them was conducted with IFFT transform and scrambled with phase factors, then signals in time-domain with minimum PAPR was chosen [17].

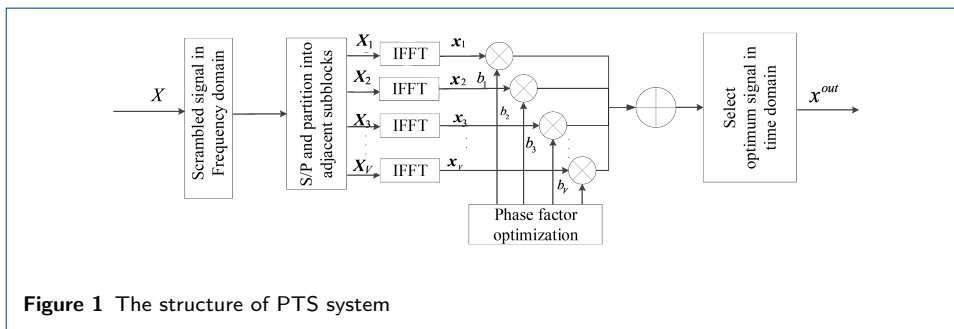
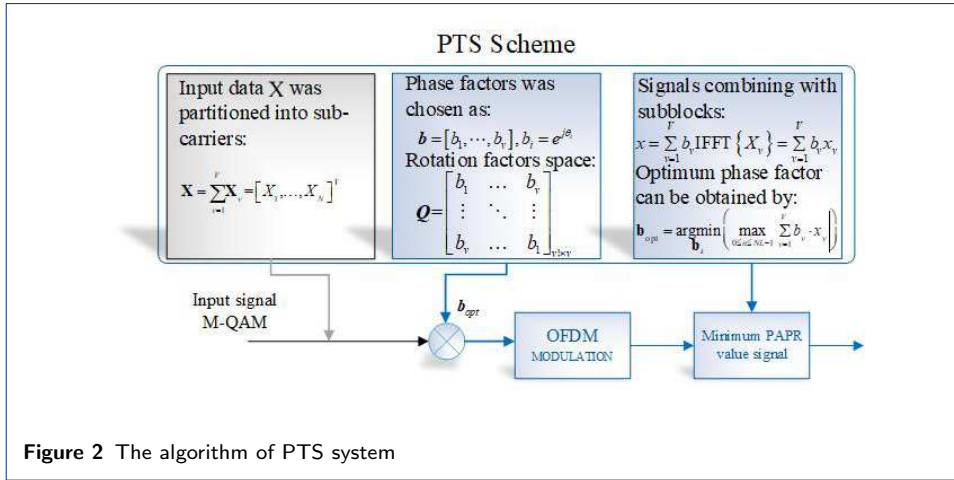


Figure 1 The structure of PTS system

The main algorithm of PTS scheme was shown in Fig. 2. Frequency domain signal \mathbf{X} is divided into V disjoint sub-blocks as $\mathbf{X}_v = [X_{v,0}, X_{v,1}, \dots, X_{v,N-1}]$, and $v = \{1, 2, \dots, V\}$. which only N/V signals are available while others are padded with 0. A random OFDM signal can be shown as follow:

$$X_v(k) = \begin{cases} X(k), & \text{if } X(k) \subseteq X_v \\ 0, & \text{if } X(k) \notin X_v \end{cases} \quad (5)$$



where $X(k)$ denotes signals appears in the v -th sub-blocks. Phase weighting factors $\mathbf{b} = [b_1, b_2, \dots, b_V]$ was achieved by $\Phi = \{e^{j\phi_1}, \dots, e^{j\phi_v}, \dots, e^{j\phi_V}\}$ where $\phi_v \in [0, 2\pi)$, which can be represented as:

$$\mathbf{b} = \left\{ b_v = e^{j2\pi v/V} \mid v = 0, 1, \dots, V-1 \right\} \quad (6)$$

Thus, the scrambled serial time domain signal could be written as:

$$\mathbf{x} = \text{IFFT} \left\{ \sum_{v=1}^V b_v \mathbf{X}_v \right\} = \sum_{v=1}^V b_v \mathbf{x}_v \quad (7)$$

where $\mathbf{x}_v = \mathbf{F}_v^{-1} \mathbf{X}_v$ is candidate signal in the time domain, \mathbf{F}_v^{-1} is the IFFT calculation padded with 0. Basically, PTS utilizes random phase factors to disperse phase distribution, so that high PAPR could be avoided.

Finally, the optimum phase factors combination with minimum PAPR is chosen as follow:

$$\mathbf{b}_{\text{opt}} = \underset{\mathbf{b}_k}{\text{argmin}} \left(\max_{0 \leq n \leq NL-1} \left| \sum_{v=1}^V b_v \cdot x_v \right| \right) \quad (8)$$

s.t. $\mathbf{b}_k = [b_1, b_2, \dots, b_v], k = 1, \dots, M$

where \mathbf{b}_{opt} is the best combination. $V!$ groups of none-repeating candidate signals can be generated, M groups of candidate signals are randomly selected from $V!$. The closer M was to $V!$, the probability removing closer to the theoretical best phase factors combinations.

To demodulate the signals at the receiver, Side Information (SI) about phase rotation factors must be sent either, the quantity of SI can be represented as: $\text{SI}^{\text{C-PTS}} = \log_2 V!$ BS, where BS is bits per sample[20].

1.2 Computational complexity and optimization of PTS

It's well known that conventional PTS scheme has extremely high computational complexity when exhaustive searched. Especially, massive IFFT calculation is an insupportable burden[21].

The complexity of random partitioning PTS when applying LN -FFT calculation can be represented as:

$$C_{add} = V(LN \log_2 LN) \quad (9)$$

and,

$$C_{mult} = V\left(\frac{LN}{2} \log_2 LN\right) \quad (10)$$

respectively, where C_{add} represents the additive computational complexity and C_{mult} represents the multiplicative computational[22].

The complexity of PTS when applying M searching space in (8) can be represented as :

$$CS_{add} = MLN(V - 1) \quad (11)$$

and,

$$CS_{mult} = MLN(V + 1) \quad (12)$$

It can be concluded from (11) and (12) that the complexity increase exponentially with the searching time M increases.

2 Low computational F-PTS

Simply put, the cause of PAPR is due to the superposition of the peak amplitude if the adjacent subcarriers, which produces a resonance like effect, it can be inferred that a frequency domain phase discretization technique would exist to reduce the probability of PAPR generation.

For dispersion evaluating, the difference of correlation R_{ab} between rotation factors is analyzed in this section. Assumed that $x_{v,n}$ from $\mathbf{x}_v = [x_{v,0}, x_{v,1}, \dots, x_{v,n}, \dots, x_{v,N-1}]^T$ is a sequence of the independent complex followed $N(0, \sigma^2/2V)$. The correlation among two random signals can be represented as:

$$R_{ab}(x'_a(m), x'_b(n)) = \frac{1}{N} \left(\sum_{k=0}^{N-1} \sum_{y=0}^{N-1} b_i^k b_l^y{}^* X'(k) X'(y)^* \exp\left(j \frac{2\pi(km - yn)}{N}\right) \right) \\ , 1 \leq i, l \leq U; 0 \leq m, n < N \quad (13)$$

where $x'_a(m)$ and $x'_b(n)$ [23] represents two random signals, $X'(k)$, $X'(y)$ represents corresponding frequency domain signals. Define $\tau = m - n$, after simplification, (13) can be written as:

$$R_{ab}(x'_a(m), x'_b(n)) = \frac{1}{N} \sum_{v=1}^V b_i^v b_l^v{}^* \sum_{k \in \mathcal{D}_v} \exp\left(j \frac{2\pi k \tau}{N}\right), -N < \tau < N \quad (14)$$

Substitute random partitioned standard $\Phi_v = \{P \text{ random independent subcarriers}\}$, and define correlation of two random signals as $R_{R,ab}(\tau)$, (14) can be transferred

into :

$$|R_{R,ab}(\tau)| \approx \begin{cases} 0 & , \tau \neq 0 \\ \frac{1}{\sqrt{V}} \cdot \left| \sum_{v=1}^V b_i^v b_i^{v*} \right| & , \tau = 0. \end{cases} \quad (15)$$

When $\tau = 0$, the correlation of two random points in identical signal can be evaluated, applying (15), the relationship of PAPR and $|R_{R,ab}(\tau)|$ was shown in Fig. 3. In general, scrambled signal with the highest PAPR is provided for reference when correlation is one, the PAPR increases with the rising of $|R_{R,ab}(\tau)|$. Since the positions of high $|R_{R,ab}(\tau)|$ signal's high-amplitude are centralized, high PAPR is inevitable. Low $|R_{R,ab}(\tau)|$ can be obtained by increasing the dispersion of phase factors. Assumed that the highest PAPR signal was chosen, whose most un-correlation signal has minimum PAPR, with large $|R_{R,ab}(\tau)|$.

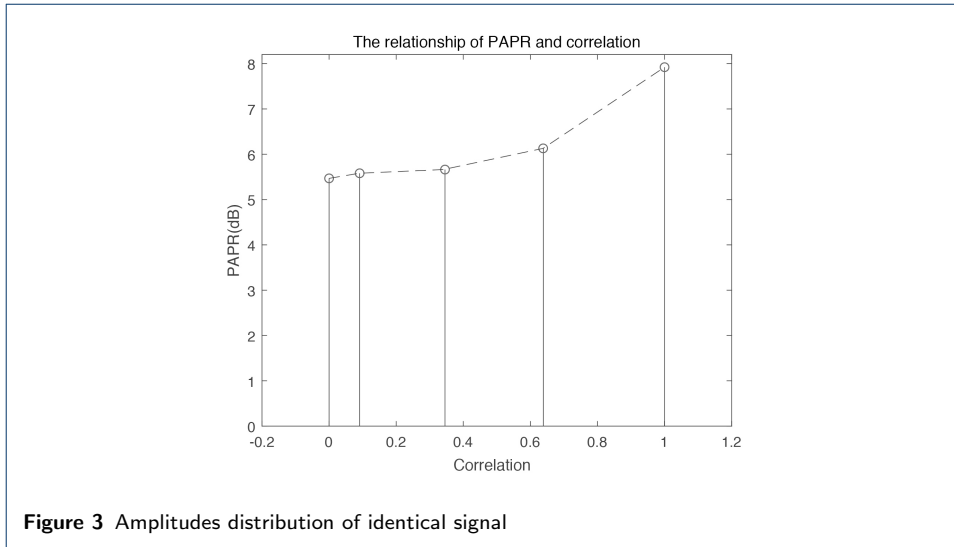


Figure 3 Amplitudes distribution of identical signal

Above-mentioned analytical result can represent the correlation characteristic in time domain only, to simply the complexity of PTS scheme, and the relationship of PAPR and frequency domain signals are discussed in follow contents. The correlation among two random signals x'_a and x'_b according to (16) can be represented as[24]:

$$\rho_{a,b} = \frac{\text{cov}(x'_a, x'_b)}{\sqrt{D(x'_a)D(x'_b)}} = \left(V - Q + \sum_{q=0}^{Q-1} S_q \right) \frac{1}{V} \quad (16)$$

where $v_q (q = 1, 2, \dots, Q)$ [25] represent two random signals. x'_a and x'_b occupy different phase factors which can be represented as:

$$\begin{cases} b_{v_q}^a \neq b_{v_q}^b & \text{if } v_q = v_1, v_2, \dots, v_q \\ b_{v_q}^a = b_{v_q}^b & \text{others} \end{cases} \quad (17)$$

$\rho_{a,b}$ is described as the correlation between two random signals; therefore, the range of $\rho_{a,b}$ can be expressed as:

$$\rho_{a,b} \geq \frac{V - 2Q}{V}, \text{ for } V \geq 2Q \quad (18)$$

where the correlation of two candidate signals $\rho_{a,b}$ mainly depends on the variety Q . Thus, the maximum $\rho_{a,b}$ is obtained when $Q=1$, which leads to the approximate PAPR.

In conclusion, the un-correlation characteristic of original signal x'_a and scrambled signal x'_b is wanted, because the probability of peak amplitude appearing in the same position of x'_a and scrambled signal x'_b can be minimize in this way.

In the F-PTS technique, dispersion evaluating in the frequency domain by SMO(Spacing Multi-Objective) optimization was adopted, candidate signal with the most dispersion phase factors was chosen.

MO optimization is widely used in various industries and has achieved remarkable success, which is aimed to find the optimum solution among multiple objectives. SMO(Spacing Multi-objective) can tackle engineering problems, which has been applied in F-PTS for phase factors dispersion evaluating[26].

Fig.5 illustrates the system model of F-PTS scheme: Signals are scrambled in frequency domain, and signal with best phase factors dispersion were chosen by SMO and send to transmitter after IFFT transmit. The operation of sub-blocks scrambling and partition can be described as:

$$\tilde{\mathbf{X}} = \sum_{v=1}^V b_v \cdot \mathbf{X}_v \quad (19)$$

where $\tilde{\mathbf{X}}$ is frequency signals after scrambling. To acquire maximum difference of signal's correlation, SMO was introduced, which can be represented as follow:

$$\begin{aligned} N &:= e, \bar{X} := \bar{d}, X_i := d_i \\ S &= \sqrt{\frac{1}{N-1}} \sum_{i=1}^N |\bar{X} - X_i| \end{aligned} \quad (20)$$

where d_i is the plural form of significant points, and \bar{X} is the mean value of all points, X_i is the i -th frequency signal from $\tilde{\mathbf{X}}$. When $S = 0$, scrambled signals reach the most discrete state, the dispersion of constellation get worse with the increasing of S . Therefore, the $V!$ combinations' dispersion can be examined as follow:

$$\begin{aligned} \tilde{\mathbf{b}}_{\text{opt}} &= \underset{\mathbf{b}_k}{\text{argmin}} \left(\sqrt{\frac{1}{N-1}} \sum_{i=1}^N |\bar{X} - X_i| \right) \\ \text{s.t. } \mathbf{b}_k &= [b_1, b_2, \dots, b_v] \\ \text{s.t. } k &= 1, \dots, V! \end{aligned} \quad (21)$$

where \tilde{b}_{opt} is the scrambled signal combination with the best dispersion.

After applied method above to evaluate the dispersion of phase factors combination in frequency domain, signal with the most discrete phase factors could be transmitted, which can be expressed as:

$$\begin{aligned} \mathbf{x} &= \text{IFFT}\{\mathbf{X}_{opt}\} \\ \mathbf{X}_{opt} &= \sum_{v=1}^V b_v \cdot \mathbf{X}_v \\ s.t. \quad b &= b_{opt} \end{aligned} \quad (22)$$

where \mathbf{X}_s is the most scrambled signal.

F-PTS applied with a spacing algorithm can be described as follow.

Algorithm 1 F-PTS with low computational complexity

Input: OFDM signal in frequency domain

Output: OFDM signal in time domain with compromise optimal PAPR reduction performance

1: **Begin**

2: Initialize the data of OFDM system

3: Generate $V!$ groups of phase factors combinations as $b_v!$

4: **for** $n = 1 : 1 : N$ **do**

5: Partition OFDM signal as: $\mathbf{X} = \sum_{v=1}^V b_v \mathbf{X}_v$

6: **for** $v = 1 : 1 : V$ **do**

7: Apply adjacent partition method

8: **end for**;

9: **end for**;

10:

11: **function** MERGER(V, x)

12: **for** $i = 1 : 1 : V!$ **do**

13: Scramble signals as: $\mathbf{X} = \sum_{v=1}^V b_v X_v$

14: Evaluate frequency-domain signal dispersion as: $Spacing(X_i) = \sqrt{\frac{1}{N-1} \sum_{i=1}^N |\bar{X} - X_i|}$

15: **end for**

16: Select signal with the best dispersion: $x_{opt} = \sum_{v=1}^V b_v \cdot x_v = \sum_{v=1}^V b_v \cdot \text{IFFT}\{X_v\}$

17: Compute per se signal PAPR as result

18: **return result**

19: **end function** $\tilde{b}_{opt} = \underset{\mathbf{b}_k}{\text{argmin}} \left(\sqrt{\frac{1}{N-1} \sum_{i=1}^N |\bar{X} - X_i|} \right) s.t. \mathbf{b}_k = [b_1, b_2, \dots, b_v] s.t. k = 1, \dots, V!$

20: Output the best dispersion with compromising optimal PAPR

21: **End**

The algorithm and structure of F-PTS is shown as Fig. 4 and Fig. 5, where F-T represents frequency domain.

The complexity of F-PTS applying with SMO algorithm can be represented as:

$$C_{f-add} = LN \cdot \log_2 LN + (V-1)V! \frac{N}{V} + V! [2O(N)] \quad (23)$$

and,

$$C_{f-mult} = V!O(N^2) + (LN/2)\log_2 LN \quad (24)$$

where $g_o = V! [2O(N) + O(N^2)]$ is complexity of SMO algorithm, addition operation and subtraction operation are both $O(N)$, quadratic operation is $O(N^2)$.

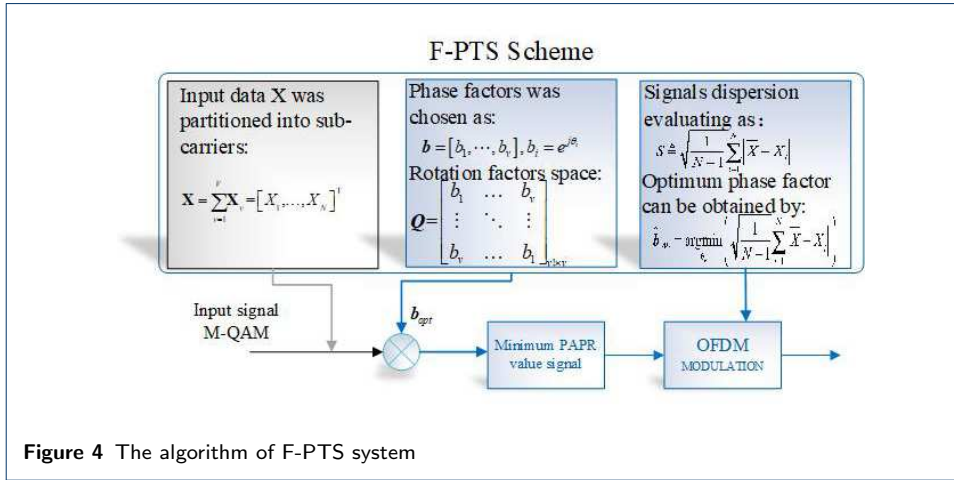


Figure 4 The algorithm of F-PTS system

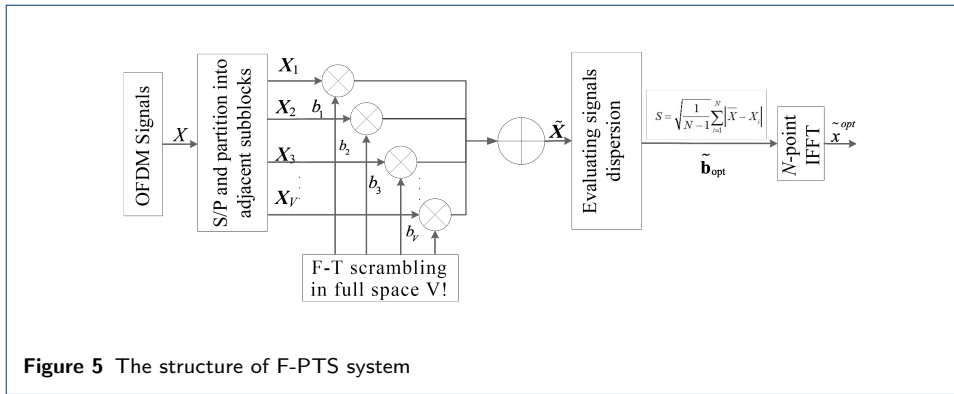


Figure 5 The structure of F-PTS system

Signals with higher frequency-domain dispersion performance has lower probability to produce high PAPR, which is considered as a suboptimal algorithm.

The proposed F-PTS scheme first chooses the scrambled signal with the highest frequency dispersion, avoid massive IFFT calculation complexity. Since peak amplitude superimposition could be avoided by dispersion evaluating, only one IFFT is required, a compromise performance could be obtained by F-PTS technique, and the complexity is dramatically reduced.

3 Frequency domain and Time domain evaluating PTS(FTD-PTS) method

Furthermore, the proposed FTD-PTS scheme aims to find optimal solution within reasonable computational complexity.

To further explore whether PAPR is only affected by $\mathbf{b} = [b_1, b_2, \dots, b_V]$, the m -th candidate signal can be expressed as:

$$\mathbf{x}_m = \sum_{v=1}^V b_v x_{v,m}, \quad m=0,1, \dots, M-1 \quad (25)$$

so that the power of signal \mathbf{x}_m can be described as:

$$\begin{aligned}
 |x_m^c|^2 &= \left| \sum_{v=1}^V b_v^c x_{v,m} \right|^2 = \left(\sum_{v=1}^V b_v^c x_{v,m} \right) \left(\sum_{v=1}^V b_v^c x_{v,m} \right)^* \\
 &= \underbrace{\sum_{v=1}^V |x_{v,m}|^2}_{\mathbf{Q}_m} + \underbrace{\sum_{\substack{v_1=1 \\ v_1 \neq v_2}}^V \sum_{v_2=1}^V (b_{v_1}^c x_{v_1,m}) (b_{v_2}^c x_{v_2,m})^*}_{\mathbf{V}_m^c}
 \end{aligned} \tag{26}$$

where $\mathbf{Q}_m = \sum_{v=1}^V |x_{v,m}|^2$ and $\mathbf{V}_m^c = \sum_{v_1=1}^V \sum_{\substack{v_2=1 \\ v_1 \neq v_2}}^V (b_{v_1}^c x_{v_1,m}) (b_{v_2}^c x_{v_2,m})^*$. $|x_m^c|^2$ can be converted into the sum of \mathbf{Q}_m and \mathbf{V}_m^c , so that (2) can be transformed as follow:

$$\text{PAPR} = 10 \log_{10} \left(\frac{\max[\mathbf{Q}_n + \mathbf{V}_m^c]}{\text{E}[|x_n|^2]} \right) \tag{27}$$

(27) shows that rotation factors and amplitude affect PAPR performance jointly.

The probability of F-PTS chooses preferred PTS subject from full space is much better than conventional PTS. In other words, x_{opt} must have good dispersion characteristic.

When only frequency-domain dispersion were considered in SMO, there was reduction of probability that high PAPR appears. A novel scheme applied in this section combined dispersion evaluation with affordable complexity, hope to obtain the optimal phase factors combination .

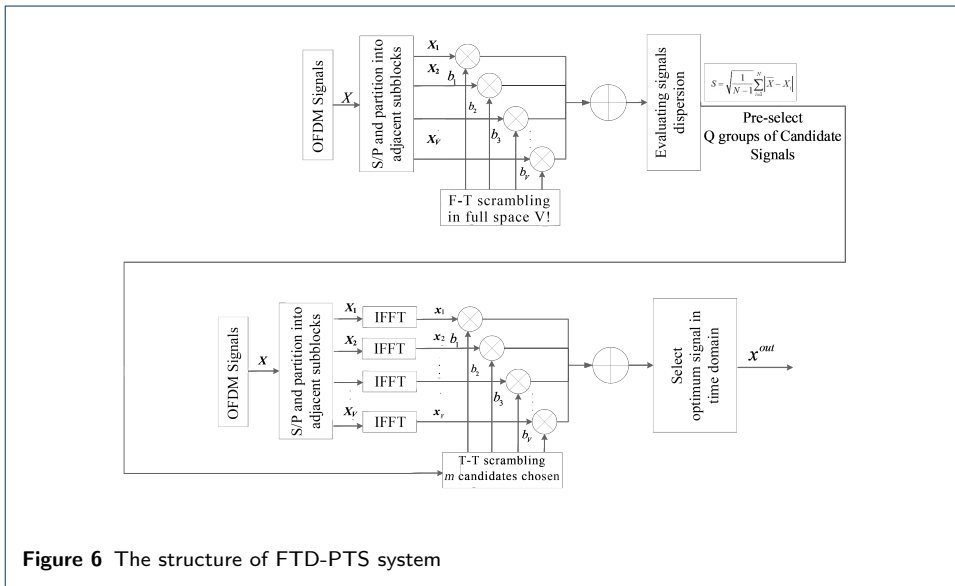


Figure 6 The structure of FTD-PTS system

FTD-PTS scheme was shown in Fig. 6, where T-T represents time domain, an frequency-domain dispersion evaluating is conducted before time-domain, Q groups included preferred PTS subject is chosen more likely, instead of randomly select M

groups. Optimal solution x_{opt} was exhausted searched after finding the preferred PTS subject was transferred into time-domain. By iteration, minimum Q was obtained to ensure that \mathbf{x}_{opt} could be chosen, and minimize the computational complexity as low as possible.

The main steps of the FTD-PTS technique are described as algorithm 2.

Algorithm 2 FTD-PTS obtain optimum PAPR reduction performance with regular computational complexity

Input: OFDM signal in frequency domain

Output: minimise PAPR(\mathbf{b}), Subject to $\mathbf{b} \in \{b_1, b_2, \dots, b_v\}$

1: **Begin**

2: Initialize the data of OFDM system

3: **for** $n = 1 : 1 : N$ **do**

4: Partition OFDM signal as: $\widehat{\mathbf{X}} = \sum_{n=1}^{V-1} \mathbf{X}_V$

5: **for** $v = 1 : 1 : V$ **do**

6: Apply adjacent partition method

7: **end for**;

8: **end for**;

9:

10: **function** MERGER(V, x)

11: **for** $i = 1 : 1 : V$ **do**

12: Scramble signals as: $\overline{\mathbf{X}} = \sum_{v=1}^V b_v \cdot \mathbf{X}_v$

13: Evaluate frequency-domain signal dispersion as: $Spacing(\mathbf{X}_i) = \sqrt{\frac{1}{N-1} \sum_{i=1}^N |\overline{\mathbf{X}} - \widehat{\mathbf{X}}_i|}$

14: **end for**

15: **for** $n = 1 : 1 : Q$ **do**

16: Scrambled OFDM signal in time-domain as: $\widehat{\mathbf{x}} = \sum_{v=1}^V b_v \text{IFFT} \{ \widehat{\mathbf{x}}_v \} = \sum_{v=1}^V b_v \widehat{\mathbf{x}}_v, s.t. [b_1, b_2, \dots, b_V] \in [b_1, \dots, b_Q]$

17: **end for**

18: Select Q groups of preferred FTD-PTS subset from full space based on SMO algorithm

19: **for** $n = 1 : 1 : Q$ **do** Search the optimal factor as: $\widehat{\mathbf{b}}_{opt} =$

$\underset{\mathbf{b}}{\text{argmin}} \left(\max_{0 \leq q \leq Q} \left| \sum_{v=1}^V b_v \cdot \widehat{\mathbf{x}}_v \right| \right), s.t. b_v \in [b_1, b_2, \dots, b_V], s.t. [b_1, b_2, \dots, b_V] \in [b_1, \dots, b_Q]$

20: **end for**

21: Select Q groups of signals with the best dispersion $Q = 1$

22: Select best combinations from Q candidate signals as FTD's PAPR

23: **while** $FTD - PAPR > C - PAPR$ **do**

24: $Q = Q + 1$

25: Select best combinations from Q candidate signals as FTD's PAPR

26: **end while**

27: Output minimum pre-select space Q

28: Compute per se signal PAPR as result

29: **return result**

30: **end function**

31: Output the best dispersion with compromising optimal PAPR

32: **End**

FTD-PTS method was illustrated as Fig.5. Initially, input signals are partitioned and scrambled as follow:

$$\widehat{\mathbf{X}} = \sum_{v=1}^V b_v \cdot \mathbf{X}_v \quad (28)$$

where $\widehat{\mathbf{X}}$ is the generated candidate signals in the frequency domain. Then the signals dispersion are evaluated, and pre-optimization Q groups of high dispersion

candidate signals as follow:

$$Spacing(\mathbf{X}_i) = \sqrt{\frac{1}{N-1}} \sum_{i=1}^N \left| \widehat{\bar{X}} - \widehat{X}_i \right| \quad (29)$$

$$[\mathbf{b}_1, \dots, \mathbf{b}_Q] = \min_{k=1}^Q \text{find} (\text{Spacing}(\widehat{\mathbf{X}}_k)) \quad (30)$$

where $\widehat{\mathbf{X}}_i$ is the i -th frequency domain signal from $\widehat{\mathbf{X}}$. As the discrete center either, $\widehat{\bar{X}}$ is the mean value of all constellations. The dispersion performance gets worse with the increasing of SMO.

Thirdly, Q groups of candidate signals are converted into disjoint sub-blocks, and scrambled with phase factors after passed IFFT blocks as follow:

$$\widehat{\mathbf{X}} = \sum_{v=1}^V \widehat{\mathbf{X}}_v \quad (31)$$

$$\begin{aligned} \widehat{\mathbf{x}} &= \sum_{v=1}^V b_v \text{IFFT} \left\{ \widehat{\mathbf{X}}_v \right\} = \sum_{v=1}^V b_v \widehat{\mathbf{x}}_v \\ \text{s.t. } [b_1, b_2, \dots, b_V] &\in [\mathbf{b}_1, \dots, \mathbf{b}_Q] \end{aligned} \quad (32)$$

Finally, search the best combinations $\widehat{\mathbf{b}}_{\text{opt}}$ from Q candidate signals. The experiment result shows that the statistical probability approach to stable when sample space is large enough, which satisfies the principle of probability.

$$\begin{aligned} \widehat{\mathbf{b}}_{\text{opt}} &= \underset{\mathbf{b}}{\text{argmin}} \left(\max_{0 \leq q \leq Q} \left| \sum_{v=1}^V b_v \cdot \widehat{x}_v \right| \right) \\ \text{s.t. } b_v &\in [b_1, b_2, \dots, b_V] \\ \text{s.t. } [b_1, b_2, \dots, b_V] &\in [\mathbf{b}_1, \dots, \mathbf{b}_Q] \end{aligned} \quad (33)$$

The flow chart of FTD-PTS can be drew as Fig 7, minimum pre-iteration space Q could be obtained by feedback.

F-PTS only conducted one IFFT calculation, and utilizing low complexity frequency-domain dispersion evaluating instead of exhausting searching in PTS, achieves extremely low complexity.

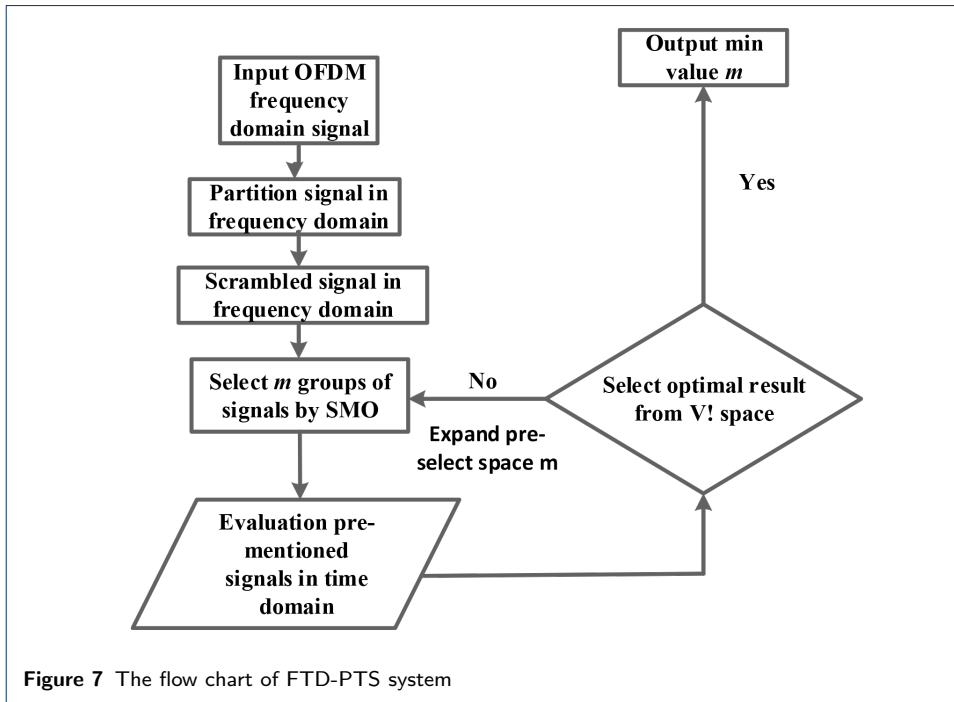
FTD-PTS maintains affordable system complexity, combined frequency-domain evaluating and Q times of best phase factors combinations searching, achieves reasonable complexity.

The complexity of FTD-PTS can be described as:

$$C_{FTD-add} = VLN \log_2 LN + (V-1)QLN + V! [2O(N)] \quad (34)$$

and,

$$C_{FTD-mult} = V(LN/2) \cdot \log_2 LN + (V-1)V! \frac{N}{2} + V!O(N^2) \quad (35)$$

**Table 1** The computational complex of multi PTS techniques.

PTS	Complex add	Complex multi
C-PTS	$V(LN/2) \cdot \log_2 LN$	$VLN \log_2 LN + (V-1)MLN$
F-PTS	$V!O(N^2) + (LN/2)\log_2 LN$	$LN \cdot \log_2 LN + (V-1)V! \frac{N}{V} + V! [2O(N)]$
FTD-PTS	$V(LN/2) \cdot \log_2 LN + (V-1)V! \frac{N}{2} + V!O(N^2)$	$VLN \log_2 LN + (V-1)QLN + V! [2O(N)]$

where $C_{FTD-add}$ and $C_{FTD-mult}$ represents the additive and multiplicative complexity respectively. FTD-PTS remains approximate complexity as PTS.

Overall, the three techniques' computational complexity is mainly concentrated on the multiplier, which F-PTS is the least, FTD-PTS and PTS are similar as expressed in Table 1.

4 Simulation results

In this chapter, PAPR reduction performance are shown for the proposed F-PTS scheme and FTD-PTS scheme. Each OFDM signal is modulated by 64 QAM, 10^5 OFDM data blocks are generated. In F-PTS, phase factors numbers are selected as $v=6$, phase partition numbers $W=V$ is the same as above, and adopted random partitioned method. Parameter setting of FTD-PTS scheme is identical as F-PTS scheme. All the simulations were completed in MATLAB. The parameters of simulations were shown in Table 2.

Table 2 Simulations parameters of Simulation results

Modulation system	OFDM
Total number of sub-carriers(N)	1024
Number of over-sampled(L)	4
Modulation method	64 QAM
Number of partition(V)	6
Number of phase factors(W)	6
Partition method	Random

To demonstrate the relationship between complexity and PAPR reduction performance, Fig. 8 compares PTS performance with different candidate signals numbers. The exhausting searching from PTS generates extremely high computational complexity. For this issue, only M times of searching was applied. The comparison of PTS performance while different M is shown as Fig 8, PAPR reduction performance ascends when the number of sub-blocks is growing, because the probability of chosen the best combinations is growing.

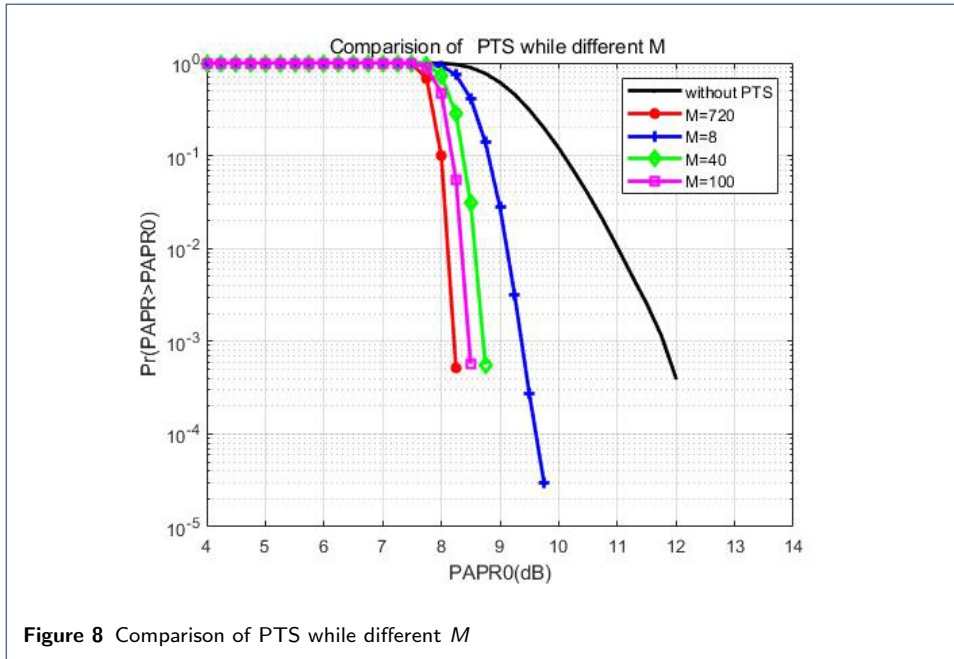


Figure 8 Comparison of PTS while different M

4.1 F-PTS simulation

Fig.9 applied $W=V=6$ phase factors, generated 720 phase combinations. The PAPR reduction from best to worst are optimal-PTS which exhaustive searched 720 phase combinations, F-PTS applied best dispersion phase combinations, PTS which searched 32 phase combinations and OFDM system without PTS with values of 7.9 dB, 8.1 dB, 8.3 dB, 11.2 dB respectively in the value of CCDF= 10^{-3} . As it shown in Fig.9, similar performance are obtained by optimal-PTS and F-PTS. For example, optimal-PTS and F-PTS with values of 8.0 dB and 8.2 dB in the value of CCDF= 10^{-2} , respectively. In the mean time, F-PTS obtained an extremely low complexity. In conclusion, F-PTS performance is better than PTS while $m=32$, and slightly inferior to PTS while $m=720$ with extremely low complexity. The complexity of F-PTS is almost 50% of PTS.

4.2 FTD-PTS simulations

Fig.10 applied $W=V=6$ phase factors, generated 720 phase combinations. The optimal-PTS were exhausted searched from full space, FTD-PTS which searched 40 phase combinations with better dispersion, FTD-PTS which searched $Q=32$ phase combinations with better dispersion, FTD-PTS which searched $Q=8$ phase

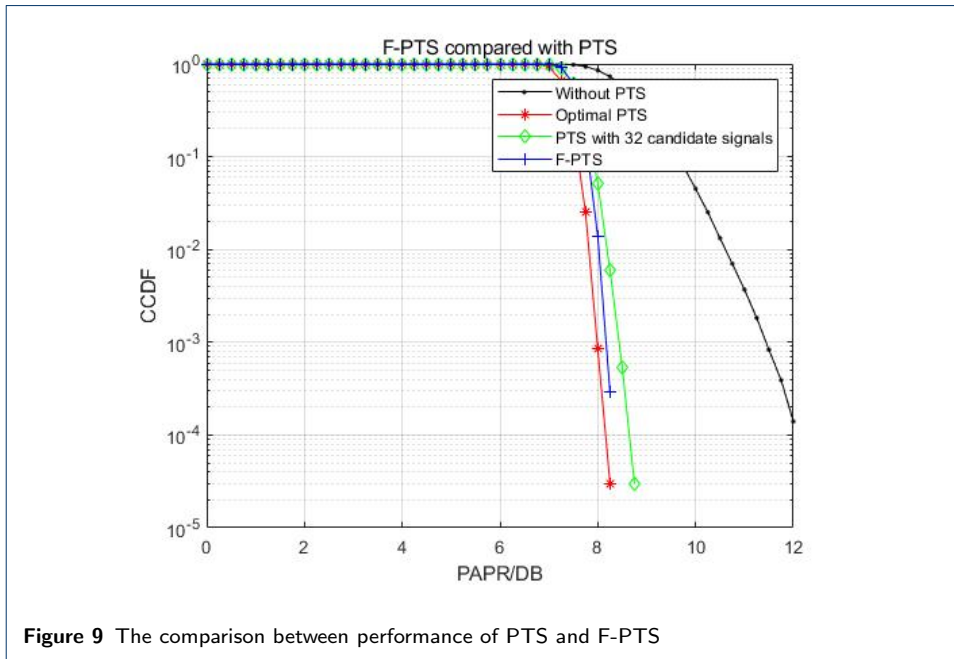


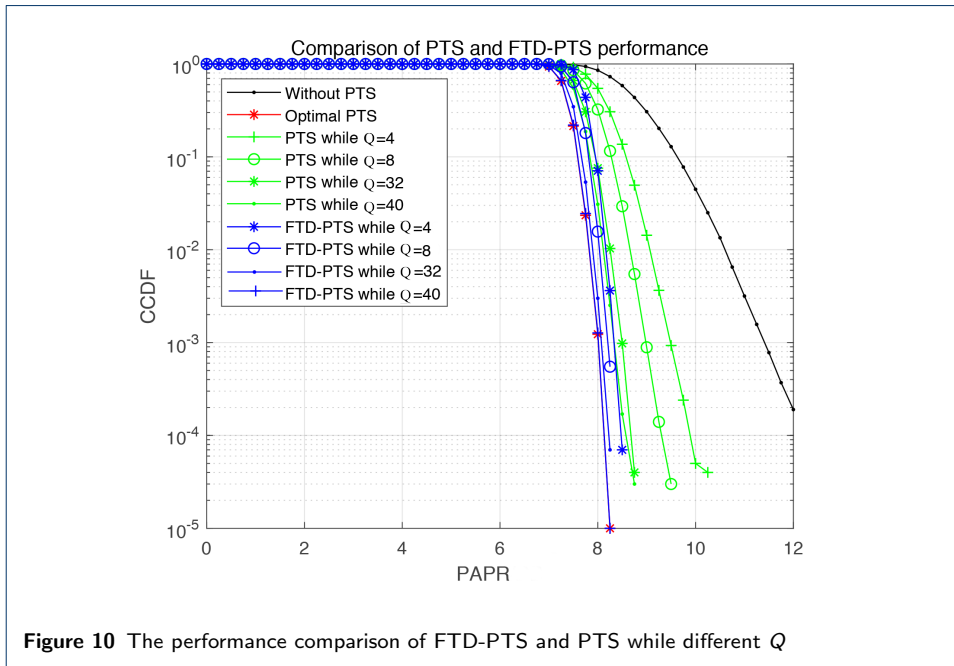
Table 3 PAPR reduction performance of PTS and F-PTS

PAPR techniques	PAPR at CCDF= e		
	$e = 10^{-2}$	$e = 10^{-3}$	$e = 10^{-4}$
PTS while $m=32$	8.2	8.3	8.4
F-PTS	8.0	8.1	-
PTS while $m=720$	7.8	7.9	8.1

combinations with better dispersion, FTD-PTS which searched $Q=4$ phase combinations with better dispersion, PTS which searched $M=40$ phase combinations, PTS which searched $M=32$ phase combinations, PTS which searched $M=8$ phase combinations, PTS which searched $M=4$ phase combinations, and OFDM system without PTS with values of 7.8 dB, 7.8 dB, 7.85 dB, 8.0 dB, 8.05 dB, 7.9 dB, 8.1 dB, 8.25 dB, 8.5 dB respectively in the value of $CCDF=10^2$. As it shown in Fig.10, almost identical performance are obtained by optimal-PTS and FTD-PTS. In the mean time, FTD-PTS obtained a reasonable complexity. In conclusion, FTD-PTS can obtained best performance within reasonable complexity.

Table 4 PAPR reduction performance of PTS while different m and FTD-PTS

PAPR techniques	PAPR at CCDF= e		
	$e = 10^{-2}$	$e = 10^{-3}$	$e = 10^{-4}$
PTS while $m=4$	8.5	8.6	8.9
PTS while $m=8$	8.25	8.5	8.8
PTS while $m=32$	8.1	8.2	8.3
PTS while $m=40$	7.9	8.0	8.25
FTD-PTS while $Q=4$	8.05	8.2	8.25
FTD-PTS while $Q=8$	8.0	8.1	-
FTD-PTS while $Q=32$	7.85	7.95	8.17
FTD-PTS while $Q=40$	7.8	7.9	8.1



5 Conclusions

This paper introduced two novel PTS techniques. F-PTS reduces the computational complexity dramatically from multiplier, maintained a compromise PAPR reduction performance. FTD-PTS adds a time-domain evaluation module to the F-PTS, and further expands the candidate signal space for dispersion evaluation. The best PAPR reduction performance can be found when the evaluation space Q is 40. FTD-PTS maintained the engineering computational complexity but reach the optimal PAPR performance, it can meet the demand of reducing papr in large data transmission system, while maintaining the system computing power, so as to achieve the demand of green communication.

Abbreviated list

Full name	Abbreviation
peak-to-average power ratio	PAPR
orthogonal frequency division multiplexing	OFDM
partial transmit sequence	PTS
selective mapping	SLM
spacing multi-objective	SMO
high-power amplifiers	HPA
bit error rate	BER
complementary cumulative distribution function	CCDF

Acknowledgements

The authors would like to express gratitude to all the editors for their efforts and feedback.

Funding

This work was supported by "the Fundamental Research Funds for the Central Universities".

Availability of data and materials

No data and materials are required.

Competing interests

The authors declare that they have no competing interests.

Authors' contributions

Feng Hu contributes to the major idea of this paper. Yuan Lu is the lead author of this paper. Libiao Jin and Jianbo Liu commented to the work, all authors approve the publication of this paper.

Author details

¹School of Information and Communication Engineering, Communication University of China, Beijing, China.

²Radio Institute, Academy of Broadcasting Science, Beijing, China.

References

1. J. Zhao, S. Ni, L. Yang, Z. Zhang, Y. Gong and X. You, "Multiband Cooperation for 5G HetNets: A Promising Network Paradigm," in *IEEE Vehicular Technology Magazine*, vol. 14, no. 4, pp. 85-93, Dec. 2019, doi: 10.1109/MVT.2019.2935793.
2. L. Peng et al., "Wideband Radiation From an Offset-Fed Split Ring Resonator With Multi-Order Resonances," in *IEEE Antennas and Wireless Propagation Letters*, vol. 17, no. 12, pp. 2198-2202, Dec. 2018, doi: 10.1109/LAWP.2018.2871040.
3. He Z , Zhou L , Chen Y , et al. Low-complexity PTS Scheme for PAPR Reduction in FBMC-OQAM Systems[J]. *IEEE Communications Letters*, 2018:1-1.
4. Chapa B P , Gottapu S R , Mogadala V K . Energy Efficient Green Mobile Communications in India by 2020[C]// *International Conference on Recent Innovations in Electrical, Electronics and Communication Engineering*. 0.
5. BIAO CAI, AIJUN LIU, AND XIAOHU LIANG. Low-Complexity Partial Transmit Sequence Methods Using Dominant Time-Domain Samples for Multicarrier Faster-Than-Nyquist Signaling. *IEEE Access*, VOLUME 7, August 27, 2019:121552-121564.
6. Zongmiao He , Lingyu Zhou, Yiou Chen, and Xiang Ling. Low-Complexity PTS Scheme for PAPR Reduction in FBMC-OQAM Systems. *IEEE COMMUNICATIONS LETTERS*, VOL. 22, NO. 11, NOVEMBER 2018:2322-2325.
7. Lopez E , Monteiro J , Carrasco P , et al. Development, implementation and evaluation of a wireless sensor network and a web-based platform for the monitoring and management of a microgrid with renewable energy sources[C]// *2019 International Conference on Smart Energy Systems and Technologies (SEST)*. 2019.
8. Mahmood A , Hossain M M A , Cavdar C , et al. Energy-Reliability Aware Link Optimization for Battery-Powered IoT Devices with Non-Ideal Power Amplifiers[J]. *IEEE Internet of Things Journal*, 2019, 6(3):5058-5067.
9. Merah H , Mesri M , Talbi L . Complexity Reduction of PTS Technique to Reduce PAPR of OFDM Signal Used in Wireless Communication System[J]. *IET Communications*, 2019, 13(7):939-946.
10. Ramteke S B , Deshmukh A Y , Dekate K N . A Review on Design and Analysis of 5G Mobile Communication MIMO System with OFDM[C]// *2018 Second International Conference on Electronics, Communication and Aerospace Technology (ICECA)*. IEEE, 2018.
11. Lv S , Zhao J , Yang L , et al. Genetic Algorithm Based Bilayer PTS Scheme for Peak-to-Average Power Ratio Reduction of FBMC/OQAM Signal[J]. *IEEE Access*, 2020, 8:17945-17955.
12. Lee K S , Kang H , No J S . New PTS Schemes With Adaptive Selection Methods of Dominant Time-Domain Samples in OFDM Systems[J]. *IEEE Transactions on Broadcasting*, 2018, 64(3):747-761.
13. Kumar P R , Naganjaneyulu P V , Prasad K S . Hybrid PS-GW optimised PTS scheme for PAPR reduction in OFDM system[J]. *IET Communications*, 2019, 13(18).
14. Jawhar Y A , Audah L , Taher M A , et al. A Review of Partial Transmit Sequence for PAPR Reduction in the OFDM Systems[J]. *IEEE Access*, 2019:1-1.
15. Pawar D S , Badodekar H S . Review of PAPR Reduction Techniques in Wireless Communication[C]// *2018 IEEE Global Conference on Wireless Computing and Networking (GCWCN)*. IEEE, 2018.
16. Ali T H , Hamza A . A novel PTS scheme based on MCAKM for peak-to-average power ratio reduction in OFDM systems[J]. *IET Communications*, 2019, 14(1).
17. Prasad S , Jayabalan R . PAPR reduction in OFDM using scaled particle swarm optimisation based partial transmit sequence technique[J]. *The Journal of Engineering*, 2019, 2019(5):3460-3468.
18. Ce J , Chao Z , Wenjing Z . Low-complexity PTS scheme based on phase factor sequences optimization[J]. *Journal of Systems Engineering and Electronics*, 2018, 29(4):707-713.
19. Moghaddam N A , Maleki A , Sharafat A R . Peak-to-Average Power Ratio Reduction in LTE-Advanced Systems Using LowComplexity and Low Delay PTS[J]. *IET Communications*, 2020, 14(11).
20. Wang Y , Zhang R , Li J , et al. PAPR Reduction Based on Parallel Tabu Search for Tone Reservation in OFDM Systems[J]. *Wireless Communications Letters*, IEEE, 2019, 8(2):576-579.
21. Tahkoubit K , Ali-Pacha A , Shaiek H , et al. Iterative Dichotomy PAPR Reduction Method for Multicarrier Waveforms[J]. *IEEE communications letters*, 2019, 23(11):2073-2076.
22. Thota S , Kamatham Y , Paidimarry C S . Analysis of Hybrid PAPR Reduction Methods of OFDM Signal for HPA Models in Wireless Communications[J]. *IEEE Access*, 2020, Volume 8(IEEE Access 2020):22780-22791.
23. Cai B , Liu A , Liang X . Low-Complexity PTS Methods Using Dominant Time-Domain Samples for MFTN Signaling[J]. *IEEE Access*, 2019, PP(99):1-1.
24. Jawhar Y A , Ramli K N , Mustapha A , et al. Reducing PAPR with low complexity for 4G and 5G waveform designs[J]. *IEEE Access*, 2019, PP(99):1-1.
25. Ahmed M S , Boussakta S , Al-Dweik A J , et al. Efficient Design of Selective Mapping and Partial Transmit Sequence using T-OFDM[J]. *IEEE Transactions on Vehicular Technology*, 2019, PP(99):1-1.
26. Tang B , Qin K , Zhang X , et al. A Clipping-Noise Compression Method to Reduce PAPR of OFDM Signals[J]. *IEEE Communications Letters*, 2019, PP(99):1-1.
27. Y.A.Al-Jawhar,K.N.Ramli,M.S.Ahmed,R.Abdulhasan,H.Farhood, and M. Alwan, "A New Partitioning Scheme for PTS Technique to Improve the PAPR Performance in OFDM Systems," *Int. J. Eng. Technol. Innov.*, vol. 8, no. 3, pp. 217-227, May 2018.

28. Kim K H . PAPR Reduction in OFDM-IM Using Multilevel Dither Signals[J]. 2018.
29. Rateb A M , Labana M . An Optimal Low Complexity PAPR Reduction Technique for Next Generation OFDM Systems[J]. IEEE Access, 2019:16406-16420.

Figures

Figure 1 The structure of PTS system. The picture illustrate the structure of PTS scheme.

Figure 2 The algorithm of PTS system. This picture illustrate the PTS algorithm by utilizing necessary formulas.

Figure 3 Amplitudes distribution of identical signal. This picture illustrate the relationship between correlation and amplitudes.

Figure 4 The algorithm of F-PTS system. This picture illustrate the F-PTS algorithm by utilizing necessary formulas.

Figure 5 The structure of F-PTS system. The picture illustrate the structure of F-PTS scheme.

Figure 6 The structure of FTD-PTS system. The picture illustrate the structure of FTD-PTS scheme.

Figure 7 The flow chart of FTD-PTS system. The picture illustrate the structure of FTD-PTS scheme by flow chart.

Figure 8 Comparison of PTS while different M. The picture shows the performance of PTS scheme while different M.

Figure 9 The comparison between performance of PTS and F-PTS. The picture compares the difference of PTS performance and F-PTS performance.

Figure 10 The performance comparison of FTD-PTS and PTS while different Q. The picture compares the difference of PTS performance and FTD-PTS performance while different Q.

Tables

Table 1 The computational complex of multi PTS techniques. This table compares the complexity of three types of PTS by complex addition and complex multiplicative respectively.

PTS	Complex add	Complex multi
C-PTS	$V(LN/2) \cdot \log_2 LN$	$VLN \log_2 LN + (V-1)MLN$
F-PTS	$V!O(N^2) + (LN/2)\log_2 LN$	$LN \cdot \log_2 LN + (V-1)V! \frac{N}{V} + V! [2O(N)]$
FTD-PTS	$V(LN/2) \cdot \log_2 LN + (V-1)V! \frac{N}{2} + V!O(N^2)$	$VLN \log_2 LN + (V-1)QLN + V! [2O(N)]$

Table 2 Simulations parameters of Simulation results. This table shows the parameters setting of this paper, while left side is the name of different settings, right side is the value setting of different parameters.

Modulation system	OFDM
Total number of sub-carriers(N)	1024
Number of over-sampled(L)	4
Modulation method	64 QAM
Number of partition(V)	6
Number of phase factors(W)	6
Partition method	Random

Table 3 PAPR reduction performance of PTS and F-PTS. This table shows the value of different schemes's PAPR while different CCDF.

PAPR techniques	PAPR at CCDF=e		
	$e = 10^{-2}$	$e = 10^{-3}$	$e = 10^{-4}$
PTS while m=32	8.2	8.3	8.4
F-PTS	8.0	8.1	-
PTS while m=720	7.8	7.9	8.1

Table 4 PAPR reduction performance of PTS while different m and FTD-PTS. This table shows the value of different schemes's PAPR while different CCDF.

PAPR techniques	PAPR at CCDF=e		
	$e = 10^{-2}$	$e = 10^{-3}$	$e = 10^{-4}$
PTS while m=4	8.5	8.6	8.9
PTS while m=8	8.25	8.5	8.8
PTS while m=32	8.1	8.2	8.3
PTS while m=40	7.9	8.0	8.25
FTD-PTS while Q=4	8.05	8.2	8.25
FTD-PTS while Q=8	8.0	8.1	-
FTD-PTS while Q=32	7.85	7.95	8.17
FTD-PTS while Q=40	7.8	7.9	8.1

Figures

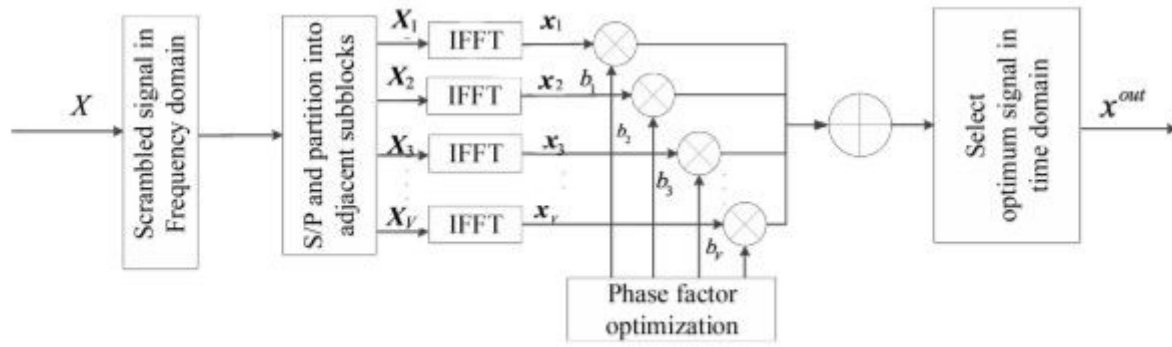


Figure 1

The structure of PTS system

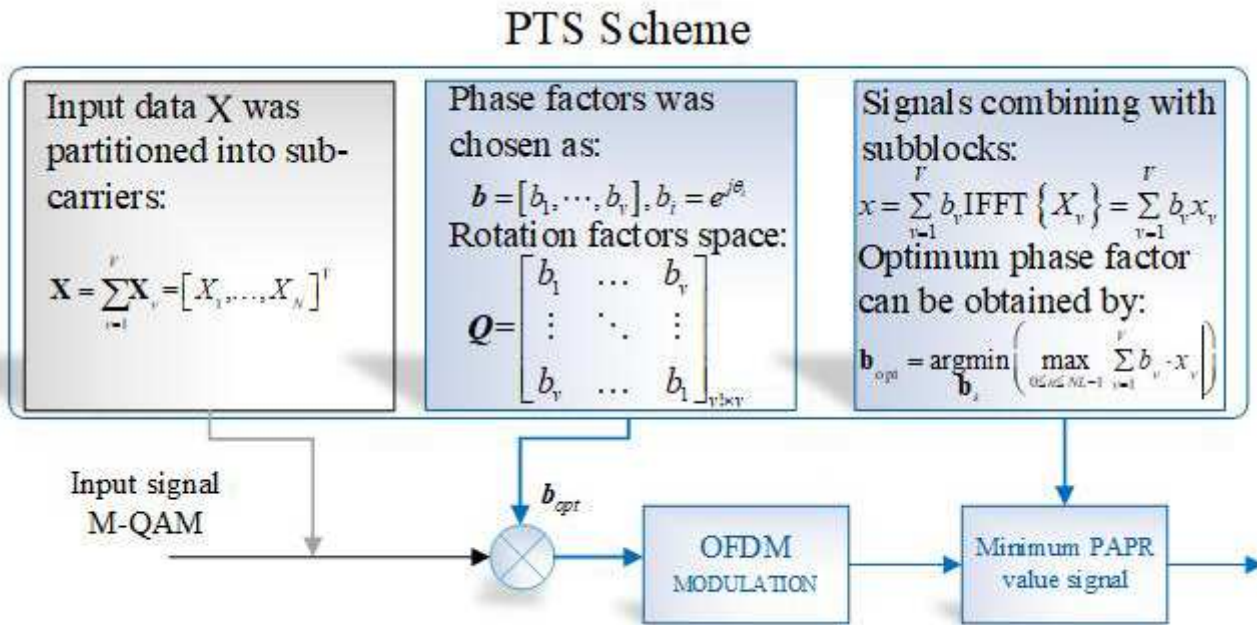


Figure 2

The algorithm of PTS system

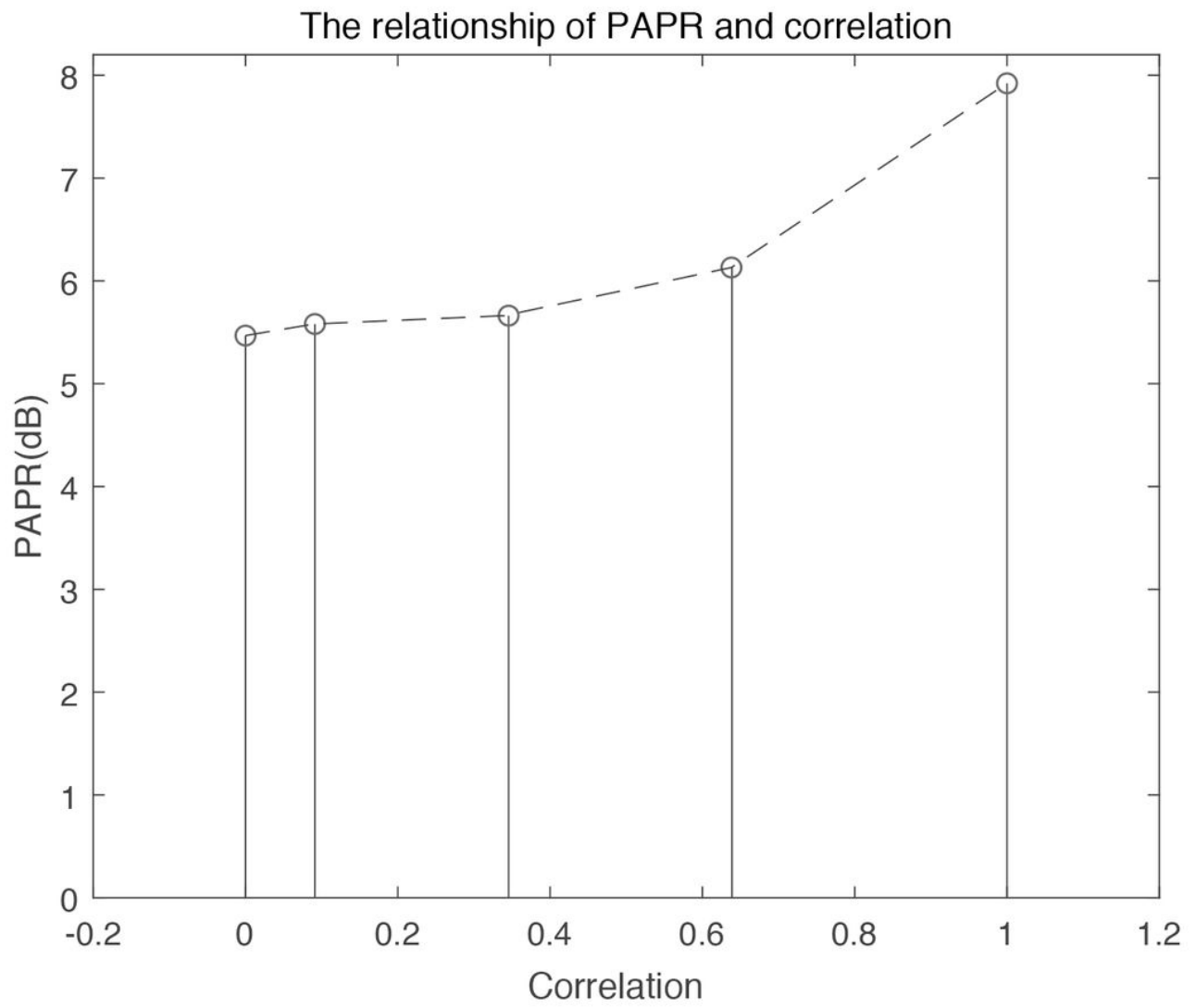


Figure 3

Amplitudes distribution of identical signal

F-PTS Scheme

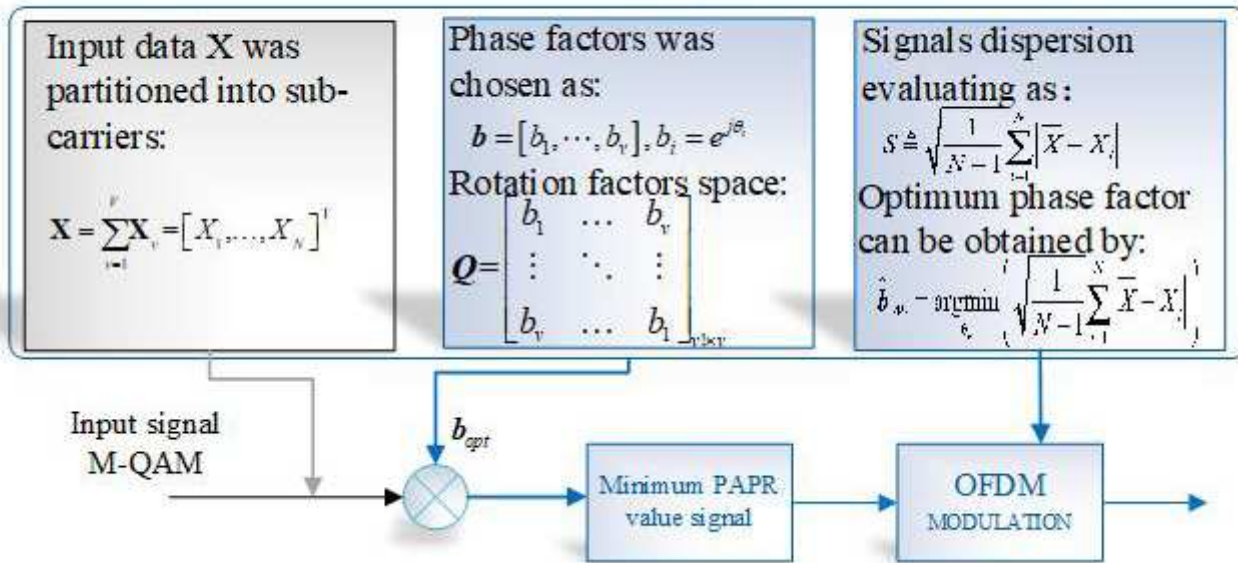


Figure 4

The algorithm of F-PTS system

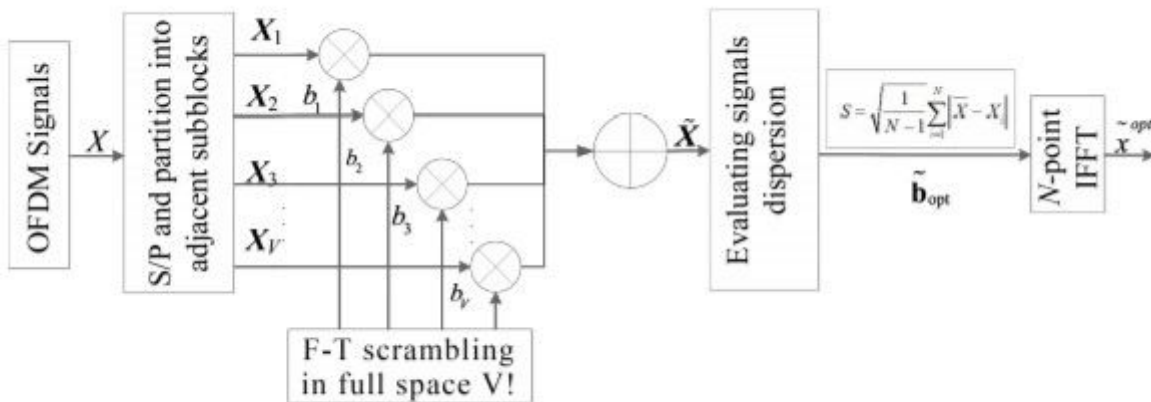


Figure 5

The structure of F-PTS system

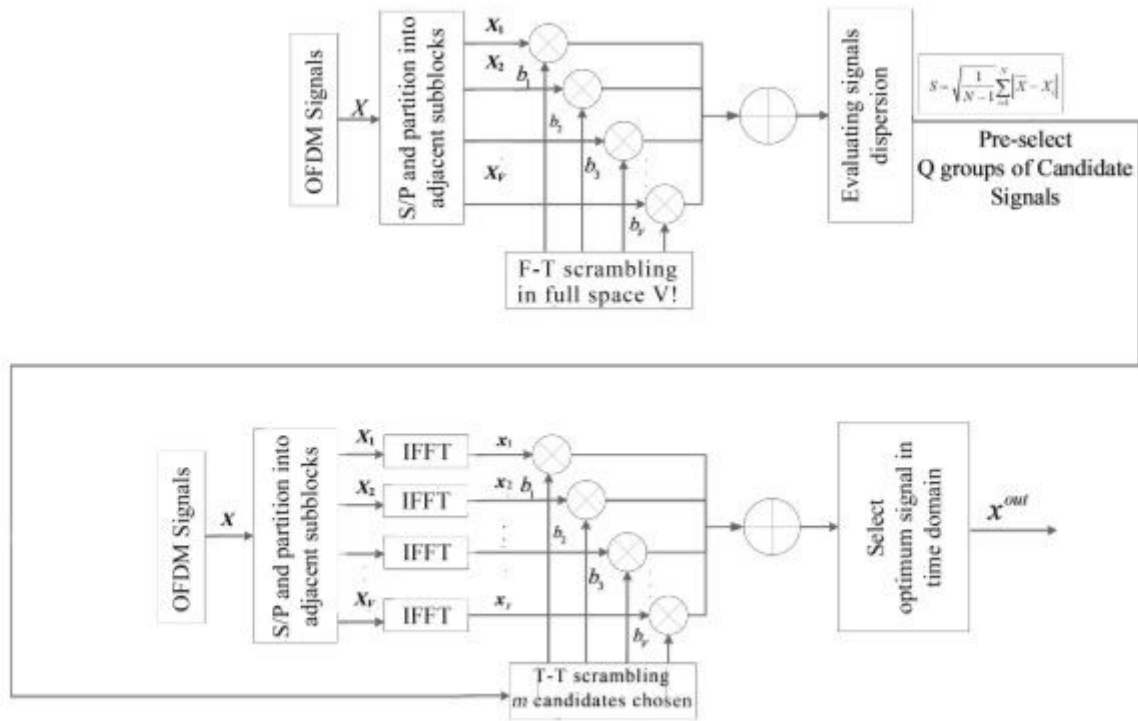


Figure 6

The structure of FTD-PTS system

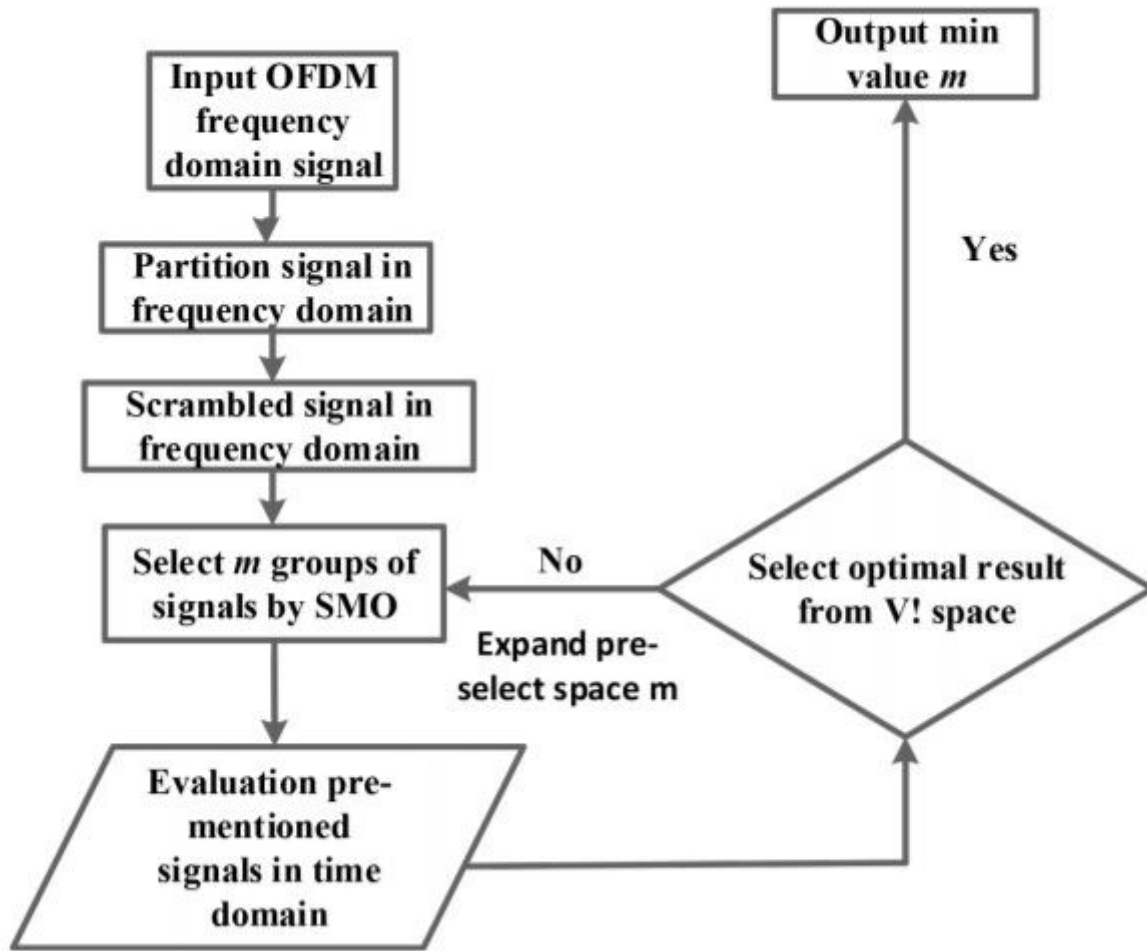


Figure 7

The flow chart of FTD-PTS system

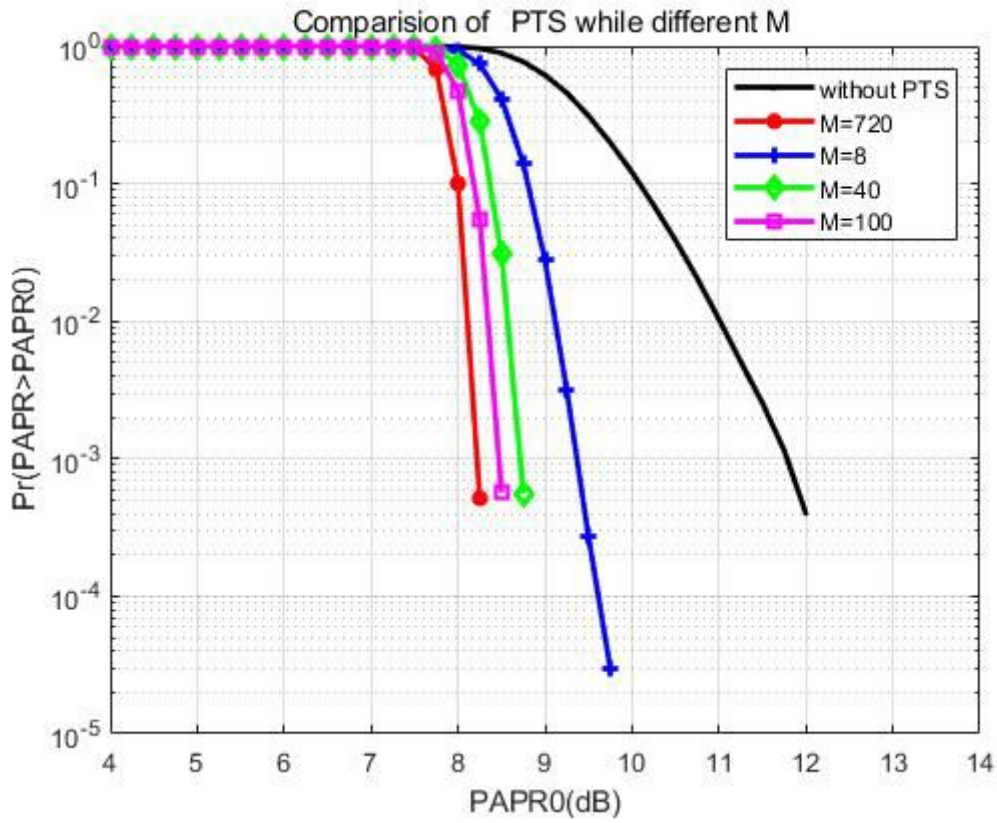


Figure 8

Comparison of PTS while different M

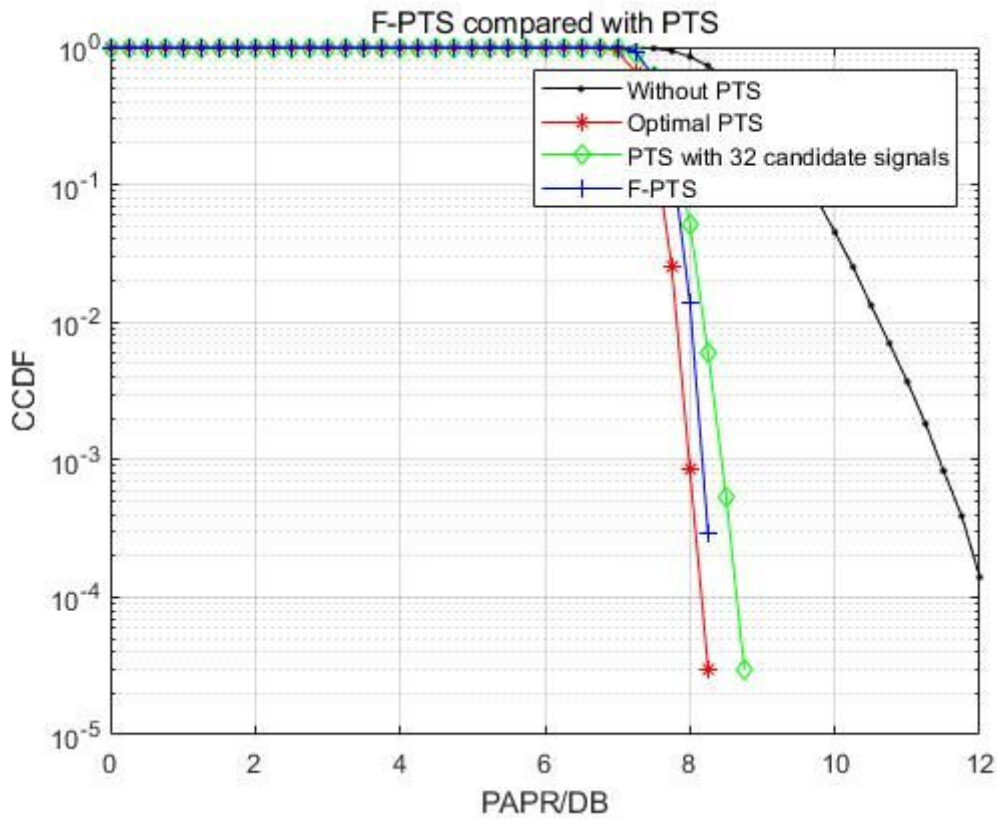


Figure 9

The comparison between performance of PTS and F-PTS

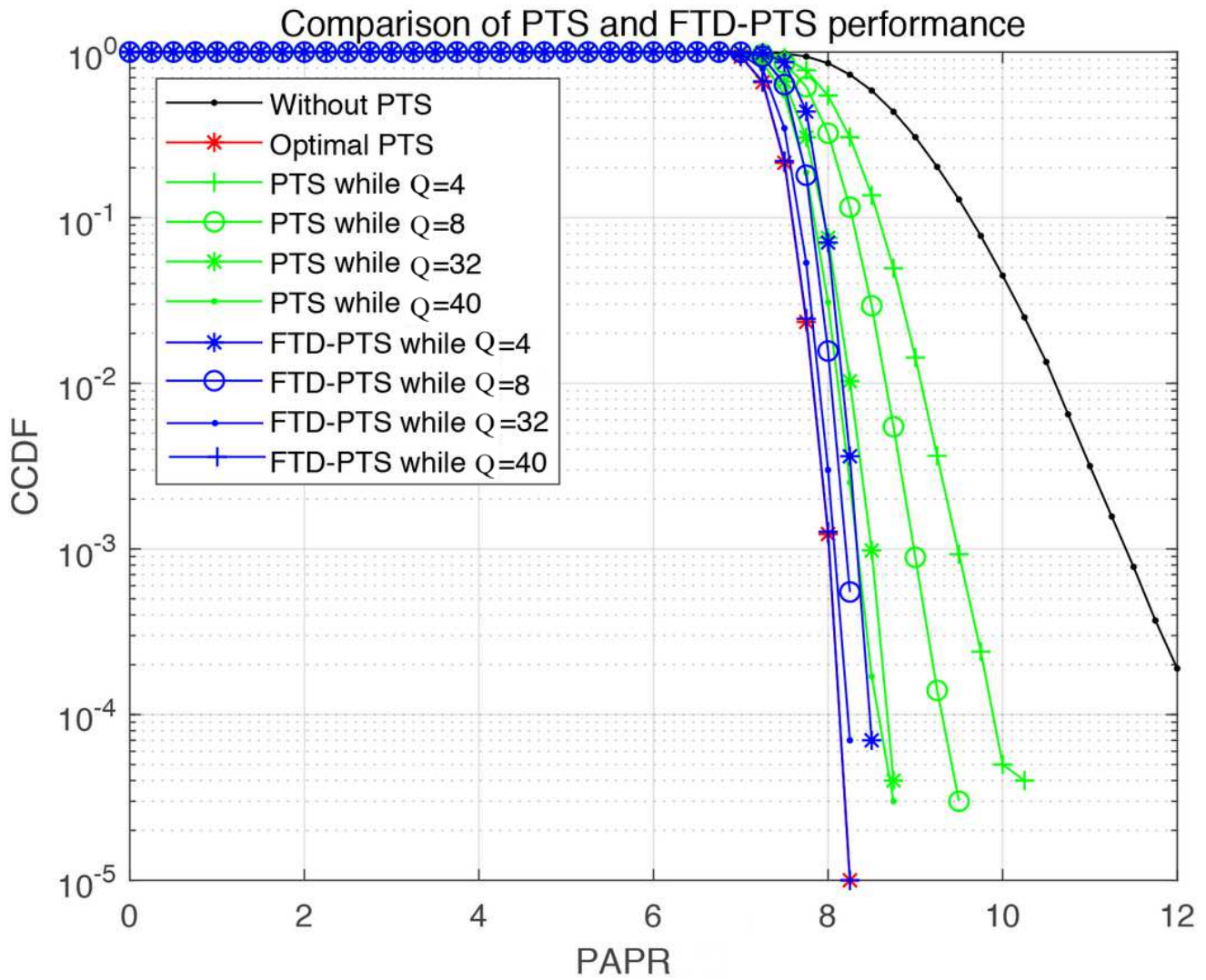


Figure 10

The performance comparison of FTD-PTS and PTS while different Q